Zwitterionic fluorinated detergents: From design to membrane protein applications

Marine Soulié, Anais Deletraz, Moheddine Wehbie, Florian Mahler, Ilham Bouchemal, Aline Le Roy, Isabelle Petit-Härtlein, Sandro Keller, Annette Meister, Eva Pebay-Peyroula, et al.

Biochimie 205 (2023) 40–52

Contents lists available at ScienceDirect

Biochimie

journal homepage: www.elsevier.com/locate/biochi

Zwitterionic fluorinated detergents: From design to membrane protein applications

Marine Soulié [a, 1], Anais Deletraz [a], Moheddine Wehbie [a], Florian Mahler [b], Ilham Bouchemal [c], Aline Le Roy [c], Isabelle Petit-Härtlein [c], Sandro Keller [b, d, e, f], Annette Meister [g], Eva Pebay-Peyroula [c], Cécile Breyton [c], Christine Ebel [c], Grégory Durand [a, *, 1]

[a] Institut des Biomolécules Max Mousseron (UMR 5247 UM-CNRS-ENSCM) & Avignon University, Equipe Chimie Bioorganique et Systèmes amphiphiles, 301 rue Baruch de Spinoza – 84916 AVIGNON cedex 9, France
[b] Molecular Biophysics, Technische Universität Kaiserslautern (TUK), Erwin-Schrödinger-Str. 13, 67663 Kaiserslautern, Germany
[c] Univ. Grenoble Alpes, CNRS, CEA, CNRS, IBS, F-38000 Grenoble, France
[d] Biophysics, Institute of Molecular Biosciences – IMB, NAWI Graz, University of Graz, Humboldtstr. 50/III, 8010 Graz, Austria
[e] Field of Excellence BioHealth, University of Graz, Graz, Austria
[f] BioTechMed-Graz, Graz, Austria
[g] Institute of Biochemistry and Biotechnology, and Interdisciplinary Research Center HALOmem, Charles Tanford Protein Center, Martin Luther University Halle-Wittenberg, Kurt-Mothes-Straße 3a, 06120 Halle/Saale, Germany

ARTICLE INFO

Article history:
Received 17 June 2022
Received in revised form
27 October 2022
Accepted 5 November 2022
Available online 11 November 2022

ABSTRACT

We report herein the synthesis of zwitterionic sulfobetaine (SB) and dimethylamine oxide (AO) detergents whose alkyl chain is made of either a perfluorohexyl (F_6H_3) or a perfluoropentyl (F_5H_5) group linked to a hydrogenated spacer arm. In aqueous solution, the critical micellar concentrations (CMCs) measured by surface tensiometry (SFT) and isothermal titration calorimetry (ITC) were found in the millimolar range (1.3–2.4 mM). The morphologies of the aggregates were evaluated by dynamic light scattering (DLS), analytical ultracentrifugation (AUC), small-angle X-ray scattering (SAXS), and transmission electron microscopy (TEM), demonstrating that the two perfluoropentyl derivatives formed small micelles less than 10 nm in diameter, whereas the perfluorohexyl derivatives formed larger and more heterogeneous micelles. The two SB detergents were able to solubilize synthetic lipid vesicles in a few hours; by contrast, the perfluoropentyl AO induced much faster solubilization, whereas the perfluorohexyl AO did not show any solubilization. All detergents were tested for their abilities to stabilize three membrane proteins, namely, bacteriorhodopsin (bR), the *Bacillus subtilis* ABC transporter BmrA, and the *Streptococcus pneumoniae* enzyme SpNOX. The SB detergents outperformed the AO derivatives as well as their hydrogenated analogs in stabilizing these proteins. Among the four new compounds, F_5H_5SB combines many desirable properties for membrane-protein study, as it is a powerful yet gentle detergent.

1. Introduction

Membrane proteins (MPs) represent 20–30% of all human proteins and constitute 60% of therapeutic targets but are currently underrepresented in the Protein Data Bank [1]. Prior to any biochemical and biophysical characterization, membrane proteins need to be extracted from their native membrane environment. Because of the insolubility of membrane proteins in aqueous solution, detergents are commonly used to extract and keep them soluble in protein/detergent complexes in which the detergent covers the hydrophobic transmembrane segments of the protein. The problems faced during this process usually come from the denaturation of the protein and from the formation of aggregates [2,3]. It is therefore of the utmost importance to develop mild detergents that allow efficient extraction of the MP while making stable complexes in which the MP retains its functional structure

* Corresponding author.
E-mail address: gregory.durand@univ-avignon.fr (G. Durand).
[1] Current address: Equipe Synthèse et Systèmes Colloïdaux Bio-organiques, Unité Propre de Recherche et d'Innovation, Avignon Université, 301 rue Baruch de Spinoza – 84 916 AVIGNON cedex 9 (France).

https://doi.org/10.1016/j.biochi.2022.11.003
0300-9084/

and dynamics.

Zwitterionic detergents, which bear both cationic and anionic groups on their polar head, present interesting properties such as high-water solubility, strong interfacial properties and high foam stability. Moreover, compared with cationic and anionic detergents, the charged groups contained in zwitterionic detergents are more distributed over the micellar surface, reducing the repulsion between the hydrophilic groups. Micellization is therefore facilitated and the critical micelle concentration (CMC) decreases as compared with detergents carrying net electric charge [4,5]. In particular, sulfobetaines (SBs) having an anionic sulfonate and a cationic quaternary ammonium group in the polar head group are zwitterionic at all physiologically relevant pH values and have shown interesting results for the extraction of MPs [6–9]. Other zwitterionic detergents that have proven useful in MP extraction are amine oxides such as lauryldimethylamine *N*-oxide (LDAO). For instance, LDAO has been successfully used to extract mammalian rhodopsin [10] and the photosynthetic reaction centers of bacterium *Rhodopseudomonas viridis* [11].

A limitation of existing zwitterionic detergents, however, is that they tend to be more denaturing than non-ionic detergents, presumably because of unspecific Coulombic interactions of their charged groups with solubilized MPs [12]. The "harsh" character of zwitterionic detergents thus correlates with their high hydrophilic/lipophilic balance (HLB). Among the various head-and-tail detergents that are commonly employed for MP extraction or stabilization, the "mild" ones have HLB values of about 12, whereas higher HLB indicates more strongly charged or larger polar heads such as those of SB-12 (*i.e.*, SB with a C12 chain) and LDAO [13].

As part of our long-term project devoted to the design of mild detergents, we hypothesized that the denaturing character of zwitterionic detergents could be attenuated by resorting to fluorinated hydrophobic chains rather than hydrogenated hydrophobic chains. Indeed, fluorinated surfactants have the unique property of being both hydrophobic and lipophobic. Therefore, they are generally non-cytolytic, as they show only weak interactions with the alkyl chains of natural lipids [14]. The non-denaturing and stabilizing character of fluorinated surfactants towards MPs has long been known [15–17], and there is a growing number of reports that show that they also exhibit detergency [18–21] and, thus, could be used to extract MPs.

In this work, we synthesized two sulfobetaine derivatives, F_6H_3SB and F_5H_5SB, as well as two dimethylamine oxide detergents, F_6H_3AO and F_5H_5AO (Fig. 1). By combining zwitterionic hydrophilic head groups and fluorinated chains, we expected to obtain sufficient detergency to solubilize and extract the MPs while retaining their native structures and functions. Micellization of the new detergents in aqueous solution was studied by surface tensiometry (SFT) and isothermal titration calorimetry (ITC), and the morphology of the aggregates was evaluated by dynamic light scattering (DLS), analytical ultracentrifugation (AUC), small-angle X-ray scattering (SAXS), and transmission electron microscopy (TEM). The potency of the compounds to solubilize lipid vesicles was further investigated. Furthermore, the new detergents were tested for the stabilization of several model MPs, including bacteriorhodopsin (bR), the *Bacillus subtilis* ABC transporter BmrA (*Bacillus* multidrug resistance ATP), and the *Streptococcus pneumoniae* SpNOX.

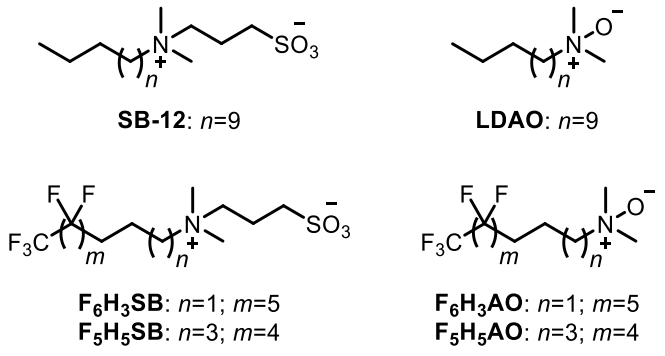

Fig. 1. Chemical structures of the commercially available SB-12 and LDAO and the four fluorinated zwitterionic derivatives synthesized in this study.

2. Materials and methods

2.1. Synthesis

All starting materials were commercially available and were used without further purification. All solvents were of reagent grade and used as received unless otherwise indicated. Anhydrous solvents were dried by simple storage over activated 4 Å molecular sieves for at least 24 h. Molecular sieves were activated by heating *in vacuo*. The progress of the reactions was monitored by thin-layer chromatography (60 F_{254} Merck plates). The compounds were detected either by exposure to ultraviolet light (254 nm) or by spraying with sulfuric acid (5% ethanol), followed by heating at ~ 150 °C. Flash column chromatography was carried out on silica gel (40–63 μm) with a CombiFlash system. ^{1}H, ^{13}C and ^{19}F NMR analyses were performed on a Bruker AC400 at 400, 100 and 375 MHz, respectively. Chemical shifts are given in ppm relative to the solvent residual peak as a heteronuclear reference for ^{1}H and ^{13}C. The coupling constants *J* are given in hertz. Abbreviations used for signal patterns are: s, singlet; bs, broad singlet; d, doublet; t, triplet; q, quartet; m, multiplet; dd, doublet of doublet; and dt, doublet of triplet. HRMS were determined on a Synapt G2-S (Waters) mass spectrometer equipped with a TOF analyzer for ESI + experiments.

***N*-(Benzyloxycarbonyl)allylamine** (**1**). Compound **1** was synthesized according to the procedure described by Olson et al. [22] Allylamine (0.56 g, 9.81 mmol, 1.0 equiv) was dissolved in H_2O (15 mL) and K_2CO_3 (4.75 g, 34.34 mmol, 3.5 equiv) was added. The mixture was stirred at room temperature for 5 min and then AcOEt (15 mL) was added and the solution was cooled down at 0 °C. Benzyl chloroformate (1.4 mL, 9.81 mmol, 1.0 equiv) was added over a period of 15 min and the reaction mixture was stirred at room temperature for 3 h. Then, the organic layer was separated, washed with a 10% HCl solution (2 ×) and brine, dried over anhydrous Na_2SO_4, filtered, and concentrated under reduced pressure. The crude product was purified by flash chromatography (AcOEt/cyclohexane, 1:9 v/v) to yield **1** as a colorless liquid (1.05 g, 56%). **1** is volatile and therefore precautions need to be taken when the solvent is evaporated. ^{1}H NMR (400 MHz, $CDCl_3$): δ 7.45-7.28 (m, 5H), 5.85 (m, 1H), 5.25-5.07 (m, 4H), 4.82 (bs, 1H), 3.83 (m, 2H). ^{13}C NMR (100 MHz, $CDCl_3$): δ 156.4, 136.6, 134.6, 128.8, 128.6, 128.2, 116.2, 66.9, 43.6. MS (ESI+) *m/z*: $[M+Na]^+ = 214.1$.

Benzyl (4,4,5,5,6,6,7,7,8,8,9,9,9-tridecafluoro-2-iodononyl) carbamate (**2**). To a solution of compound **1** (2.10 g, 10.98 mmol, 1.0 equiv) in CH_2Cl_2, perfluorohexyliodide (4.0 mL, 18.48 mmol, 1.7 equiv) and triethylborane 1 M in hexane (3.1 mL, 3.14 mmol, 0.3 equiv) were added. The mixture was flushed with air and stirred at room temperature overnight. After completion of the reaction, a diluted solution of $Na_2S_2O_3$ was added and the aqueous layer was extracted with CH_2Cl_2 (3 ×). The organic fractions were collected, dried over anhydrous Na_2SO_4, filtered, and then concentrated under reduced pressure. The crude product was purified by flash chromatography (AcOEt/cyclohexane, 1:9 v/v) to yield **2** as a white powder (5.70 g, 82%). ^{1}H NMR (400 MHz, $CDCl_3$): δ 7.40-7.30 (m, 5H), 5.21 (bs, 1H), 5.13 (s, 2H), 4.40 (m, 1H), 3.67 (m, 1H), 3.53 (m,

1H), 2.82 (m, 2H). ^{19}F NMR (375 MHz, $CDCl_3$): δ −80.8, −113.1, −121.8, −122.8, −123.5, −126.1. ^{13}C(^{1}H) NMR (100 MHz, $CDCl_3$): δ 156.3, 136.2, 128.7, 128.5, 128.3, 67.4, 49.4, 38.8, 18.5. HRMS (ESI+) *m/z*: $[M+H]^+$ calculated for $C_{17}H_{14}F_{13}INO_2$ 637.9856, found 637.9872.

Benzyl (4,4,5,5,6,6,7,7,8,8,9,9,9-tridecafluorononyl)carbamate (**3**). Compound **2** (5.70 g, 8.95 mmol, 1.0 equiv) was dissolved in MeOH and Pd/C (100 mg, catalytic amount) and sodium acetate (2.93 g, 35.72 mmol, 4.0 equiv) were added. The reaction mixture was stirred overnight under a 6.5 bar pressure of H_2 in a hydrogenation reactor and then filtered through a pad of Celite and concentrated under reduced pressure. A diluted solution of $Na_2S_2O_3$ was added to the crude product and extracted with CH_2Cl_2 (3 ×). The organic fractions were collected, dried over anhydrous Na_2SO_4, filtered, and concentrated under reduced pressure to yield **3** as a white powder (3.60 g, 79%). ^{1}H NMR (400 MHz, $CDCl_3$): δ 7.40-7.28 (m, 5H), 5.11 (s, 2H), 4.84 (bs, 1H), 3.30 (m, 2H), 2.12 (m, 2H), 1.84 (m, 2H). ^{13}F NMR (375 MHz, $CDCl_3$): δ - 80.8, −114.1, −121.9, −122.9, −123.4, −126.1. ^{13}C(^{1}H) NMR (100 MHz, $CDCl_3$): δ 156.6, 136.5, 128.7, 128.4, 128.3, 67.0, 40.3, 28.4, 21.4. HRMS (ESI+) *m/z*: $[M+H]^+$ calculated for $C_{17}H_{15}F_{13}NO_2$ 512.0890, found 512.0903.

4,4,5,5,6,6,7,7,8,8,9,9,9-tridecafluoro-*N,N*-dimethylnonan-1-amine (**4**). Compound **3** (3.60 g, 7.04 mmol, 1.0 equiv) was dissolved in MeOH and Pd/C (100 mg, catalytic amount) was added. The reaction mixture was stirred overnight under a 6.5 bar pressure of H_2 in a hydrogenation reactor and then filtered through a pad of Celite and concentrated under reduced pressure. The obtained product was dissolved in a mixture of formaldehyde and formic acid (1:2 v/v, 12 mL). To the resulting solution H_2O (2 mL) and MeOH (1 mL) were added. The reaction mixture was stirred at reflux for 24 h and then poured into NaOH 2 N. The aqueous layer was extracted with Et_2O (3 ×). The organic fractions were collected, dried over anhydrous Na_2SO_4, filtered, and concentrated under reduced pressure to yield **4** as a yellow oil (2.21 g, 77%). **4** is volatile and therefore precautions need to be taken when the solvent is evaporated. ^{1}H NMR (400 MHz, $CDCl_3$): δ 2.33 (t, J = 7.0 Hz, 2H), 2.21 (s, 6H), 2.13 (m, 2H), 1.76 (m, 2H). ^{13}F NMR (375 MHz, $CDCl_3$): δ - 80.9, - 114.3, - 122.0, - 122.9, - 123.5, - 126.2. ^{13}C(^{1}H) NMR (100 MHz, $CDCl_3$): δ 58.6, 45.4, 28.9, 18.5. HRMS (ESI+) *m/z*: $[M+H]^+$ calculated for $C_{11}H_{13}F_{13}N$ 406.0835, found 406.0848. The spectral data were in agreement with those from Ref. [23].

4,4,5,5,6,6,7,7,8,8,9,9,9-tridecafluoro-*N,N*-dimethylnonan-1-amine oxide (**5**). Compound **4** (0.80 g, 1.97 mmol, 1.0 equiv) was dissolved in $CHCl_3$ and the resulting mixture was cooled down to −10 °C using liquid nitrogen. m-CPBA (0.68 g, 3.94 mmol, 2.0 equiv) was dissolved in $CHCl_3$ and then added slowly to the reaction mixture. The reaction mixture was stirred 30 min at − 10 °C and then overnight at room temperature. The solvent was removed under reduced pressure and the crude product was recrystallized from Et_2O to yield **5** as a white solid (0.36 g, 43%). ^{1}H NMR (400 MHz, CD_3OD): δ 3.39 (m, 2H), 3.19 (s, 6H), 2.34 (m, 2H), 2.20 (m, 2H). ^{19}F NMR (375 MHz, CD_3OD): δ − 82.4, −115.4, −122.9, −123.9, −124.5, −127.4. ^{13}C(^{1}H) NMR (400 MHz, CD_3OD): δ 70.0, 58.6, 29.0, 16.0. HRMS (ESI+) *m/z*: $[M+H]^+$ calcd for $C_{11}H_{13}F_{13}NO$, 422.0790; found, 422.0793.

3-(dimethyl(4,4,5,5,6,6,7,7,8,8,9,9,9-tridecafluorononyl) ammonio)propane-1-sulfonate (**6**). Compound **4** (0.80 g, 1.97 mmol, 1.0 equiv) and 1,3-propanesultone (0.84 g, 6.90 mmol, 3.5 equiv) were dissolved in anhydrous ACN. The reaction mixture was stirred at 75 °C for 6 h under an argon atmosphere. The mixture was allowed to cool down to room temperature and then AcOEt was added. The solution was cooled down to 0 °C. The obtained precipitate was filtered, washed with Et_2O, and dried to yield **6** as a white solid (0.80 g, 77%). ^{1}H NMR (400 MHz, CD_3OD): δ 3.57 (m, 2H), 3.45 (m, 2H), 3.14 (s, 6H), 2.88 (t, J = 6.4 Hz, 2H), 2.34 (m, 2H), 2.18 (m, 4H). ^{19}F NMR (375 MHz, CD_3OD): δ 82.4, −115.2, −122.9, −123.9, −124.5, −127.3. ^{13}C(^{1}H) NMR (100 MHz, CD_3OD): δ 64.3, 64.0, 51.3, 48.2, 28.5, 19.9, 15.4. HRMS (ESI+) *m/z*: $[M+H]^+$ calcd for $C_{14}H_{19}F_{13}NO_3S$, 528.0878; found, 528.0879. The spectral data were in agreement with those from Ref. [23].

6,6,7,7,8,8,9,9,10,10,10-undecafluoro-4-iododecan-1-ol (**7**). To a solution of pent-4-en-1-ol (1.00 g, 11.61 mmol, 1.0 equiv) in CH_2Cl_2, perfluoropentyliodide (5.97 g, 15.09 mmol, 1.3 equiv) and triethylborane 1 M in hexane (3.0 mL, 3.02 mmol, 0.2 equiv) were added. The mixture was flushed with air and stirred at room temperature for 2 h. After completion of the reaction, a diluted solution of $Na_2S_2O_3$ was added and the aqueous layer was extracted with CH_2Cl_2 (3 ×). The organic fractions were collected, dried over anhydrous Na_2SO_4, filtered, and then concentrated under reduced pressure. The crude product was purified by flash chromatography (cyclohexane/AcOEt, 9:1 v/v) to yield **7** as a yellow oil (4.90 g, 88%). ^{1}H NMR (400 MHz, $CDCl_3$): δ 4.38 (m, 1H), 3.72 (t, J = 6.2 Hz, 2H), 2.86 (m, 2H), 1.88 (m, 3H), 1.70 (m, 1H). ^{19}F NMR (375 MHz, $CDCl_3$): δ −80.8, −113.2, −122.6, −123.8, −126.3. ^{13}C(^{1}H) NMR (100 MHz, $CDCl_3$): δ 61.8, 41.8, 37.0, 32.7, 20.3. HRMS (ESI+) *m/z*: $[M\text{-}H_2O + H]^+$ calcd for $C_{10}H_{19}F_{11}I$, 464.9568; found, 464.9560.

6,6,7,7,8,8,9,9,10,10,10-undecafluorodecan-1-ol (**8**). Compound **7** (4.70 g, 9.75 mmol, 1.0 equiv) was dissolved in MeOH and Pd/C (100 mg, catalytic amount) and sodium acetate (2.50 g, 30.49 mmol, 3.1 equiv) were added. The reaction mixture was stirred overnight under a 6.5 bar pressure of H_2 in a hydrogenation reactor and then filtered through a pad of Celite and concentrated under reduced pressure. A diluted solution of $Na_2S_2O_3$ was added to the crude product and extracted with CH_2Cl_2 (3 ×). The organic fractions were collected, dried over anhydrous Na_2SO_4, filtered, and concentrated under reduced pressure to yield **8** as a yellow oil (3.28 g, 94%). **8** is volatile and therefore precautions need to be taken when the solvent is evaporated. ^{1}H NMR (400 MHz, $CDCl_3$): δ 3.66 (t, J = 6.4 Hz, 2H), 2.07 (m, 2H), 1.62 (m, 4H), 1.48 (m, 2H). ^{19}F NMR (375 MHz, $CDCl_3$): δ −80.9, −114.5, −122.8, −123.8, −126.4. ^{13}C(^{1}H) NMR (100 MHz, $CDCl_3$): δ 62.6, 32.4, 31.0, 25.5, 20.1. HRMS (ESI+) *m/z*: $[M\text{-}H_2O + H]^+$ calcd for $C_{10}H_{10}F_{11}$, 339.0601; found, 339.0614.

6,6,7,7,8,8,9,9,10,10,10-undecafluorodecyl methanesulfonate (**9**). To a solution of **8** (2.7 g, 7.58 mmol, 1.0 equiv) in CH_2Cl_2, triethylamine (1.53 g, 15.12 mmol, 2.0 equiv) was added. The reaction mixture was cooled down to 0 °C and MsCl (2.60 g, 22.70 mmol, 3.0 equiv) was added dropwise. The mixture was stirred at room temperature for 6 h and then poured into water and extracted with CH_2Cl_2 (3 ×). The organic fractions were collected and successively washed with 1 M HCl and brine, dried over anhydrous Na_2SO_4, filtered and then concentrated under reduced pressure to yield **9** as a yellow oil (2.80 g, 85%). ^{1}H NMR (400 MHz, $CDCl_3$): δ 4.24 (t, J = 6.3 Hz, 2H), 3.01 (s, 3H), 2.08 (m, 2H), 1.80 (m, 2H), 1.66 (m, 2H), 1.53 (m, 2H). ^{19}F NMR (375 MHz, $CDCl_3$): δ −80.8, −114.4, −122.7, −123.7, −126.3. ^{13}C(^{1}H) NMR (100 MHz, $CDCl_3$): δ 69.5, 37.6 30.8, 29.0, 25.2, 19.9. HRMS (ESI+) *m/z*: $[M+H]^+$ calcd for $C_{11}H_{13}F_{11}O_3S$, 435.0486; found, 435.0479.

6,6,7,7,8,8,9,9,10,10,10-undecafluoro-*N,N*-dimethyldecan-1-amine (**10**). To a solution of dimethylamine (0.40 g, 8.98 mmol, 3.0 equiv) in EtOH, compound **9** (1.3 g, 2.99 mmol, 1.0 equiv) in EtOH was added. The reaction mixture was stirred at 50 °C for 24 h and then concentrated under reduced pressure. The resulting crude was poured into a solution of NaOH 1 N and extracted with Et_2O (3 ×). The organic fractions were collected, washed with brine, dried, filtered and concentrated under reduced pressured. The crude product was purified by flash chromatography (AcOEt/cyclohexane, 7:3 v/v) to yield **10** as a yellow oil (0.60 g, 53%). **10** is volatile and therefore precautions need to be taken when the solvent is

evaporated. ^{1}H NMR (400 MHz, $CDCl_3$): δ 2.26 (t, $J = 7.1$ Hz, 2H), 2.21 (s, 6H), 2.06 (m, 2H), 1.64 (m, 2H), 1.50 (m, 2H), 1.41 (m, 2H). ^{19}F NMR (375 MHz, $CDCl_3$): δ −80.3, −114.4, −122.8, −123.8, −126.3. ^{13}C(^{1}H) NMR (100 MHz, $CDCl_3$): δ 59.5, 45.4, 31.0, 27.3, 27.1, 20.2. HRMS (ESI+) *m/z*: $[M+H]^+$ calcd for $C_{12}H_{16}F_{11}N$, 384.1180; found, 384.1187.

6,6,7,7,8,8,9,9,10,10,10-undecafluoro-*N*,*N*-dimethyldecan-1-amine oxide (**11**). At 0 °C, compound **10** (0.60 g, 1.57 mmol, 1.0 equiv) was added dropwise to a solution of 30% wt. H_2O_2 in H_2O (1.00 g, 29.41 mmol, 18.7 equiv). The reaction mixture was stirred at 0 °C for 5 min, heated to 30 °C for 30 min and then concentrated under reduced pressure at 50 °C. The final product was dissolved in H_2O and lyophilized to yield **11** as a white solid. (0.55 g, 88%). ^{1}H NMR (400 MHz, CD_3OD): δ 3.28 (m, 2H), 3.16 (s, 6H), 2.22 (m, 2H), 1.90 (m, 2H), 1.70 (m, 2H), 1.48 (m, 2H). ^{19}F NMR (375 MHz, CD_3OD): δ −82.5, −115.4, −123.8, −124.8, −127.5. ^{13}C(^{1}H) NMR (100 MHz, CD_3OD): δ 71.4, 58.4, 31.5, 27.0, 24.1, 21.1. HRMS (ESI+) *m/z*: $[M+H]^+$ calcd for $C_{12}H_{16}F_{11}NO$, 400.1136; found, 400.1134.

3-(dimethyl(6,6,7,7,8,8,9,9,10,10,10-undecafluorodecyl) ammonio)propane-1-sulfonate (**12**). Compound **10** (0.80 g, 2.09 mmol, 1.0 equiv) and 1,3-propanesultone (0.89 g, 7.31 mmol, 3.5 equiv) were dissolved in anhydrous ACN. The reaction mixture was stirred at 75 °C for 6 h under an argon atmosphere. The mixture was allowed to cool to room temperature and then AcOEt was added. The solution was cooled down to 0 °C. The obtained precipitate was filtered, washed with AcOEt and Et_2O, and dried to yield **12** as a white solid (0.82 g, 78%). ^{1}H NMR (400 MHz, CD3OD): δ 3.52 (m, 2H), 3.34 (m, 2H), 3.10 (s, 6H), 2.87 (t, $J = 6.7$, 2H), 2.23 (m, 4H), 1.87 (m, 2H), 1.73 (m, 2H), 1.50 (m, 2H). ^{19}F NMR (375 MHz, CD_3OD): δ −82.5, −115.4, −123.8, −124.7, −127.5. ^{13}C(^{1}H) NMR (100 MHz, CD_3OD): δ 65.1, 63.8, 51.3, 31.5, 26.8, 23.3, 21.0, 19.9. HRMS (ESI+) *m/z*: $[M+H]^+$ calcd for $C_{15}H_{22}F_{11}NO_3S$, 506.1227; found, 506.1223.

2.2. Colloidal properties

2.2.1. Surface tension measurement (SFT)

The surface activity of detergents in solution at the air/water interface was determined using a K100 tensiometer (Kruss, Hamburg, Germany). Surface tensions were determined by dilution of stock solutions of F_6H_3SB (9.4 mM), F_5H_5SB (10 mM), F_6H_3AO (8 mM), and F_5H_5AO (7 mM) using the Wilhelmy plate technique. In a typical experiment, 8 to 13 concentration steps were prepared from solutions equilibrated overnight before measurement. All measurements were performed at (25.0 ± 0.5) °C until standard deviation reached 0.05 mN/m or during at least 30 min.

2.2.2. Isothermal titration calorimetry (ITC)

All experiments were performed on a VP-ITC (Malvern Panalytics, Malvern, UK) at 25 °C. Stock solutions of 20 mM F_6H_3SB, 30 mM F_5H_5SB, 15 mM F_6H_3AO, and 20 mM F_5H_5AO were prepared in phosphate buffer (10 mM NaH_2PO_4/Na_2HPO_4 and 150 mM NaCl at pH 7.4) and were injected into the sample cell containing only phosphate buffer. Time spacings between injections were chosen long enough to allow for complete re-equilibration. The resulting thermograms were baseline-subtracted, and peaks were integrated to yield demicellization isotherms using NITPIC [24]. Further, demicellization isotherms were analyzed using D/STAIN [25] giving the CMC, thermodynamic parameters, and corresponding 95% confidence intervals.

2.2.3. Dynamic light scattering (DLS)

DLS measurements were carried out with a Nano Zetasizer S90 (Malvern Panalytics, Malvern, UK), utilizing a He–Ne laser at a wavelength of 633 nm as light source and a detection angle of 90°. Samples were transferred to a 45-μL quartz glass cuvette (Hellma, Munich, Germany) and equilibrated for 2 min prior to each measurement. The attenuator was fixed to the maximum open position to ensure comparable results for light scattering intensity measurements while in case of the determination of size distributions, attenuator settings were automatically set by the software.

2.2.4. Sedimentation velocity experiments

Stock solutions at 50 mM were diluted in water to provide samples of F_6H_3SB at 4, 8.1 and 12 mM, of F_5H_5SB at 3.9 and 8 mM, of F_6H_3AO at 3.7, 6.1 and 13.2 mM, and of F_5H_5AO at 3, 5, 10.9, and 15.5 mM. Sedimentation velocity experiments were performed in a Beckman XL-I analytical ultracentrifuge with a rotor Anti-50 (Beckman Coulter, Palo Alto, USA) and double-sector cells of optical path length 12 mm equipped of Sapphire windows (Nanolytics, Potsdam, Germany). Samples were centrifuged at 42 000 rpm (130 000 *g*), at 20 °C. Sedimentation velocity profiles were acquired in interference, every 1 min. Data were analyzed in terms of continuous size distribution c(s) of sedimentation coefficients, *s* [26], by using SEDFIT. Peak integration was done with the GUSSI software (http://biophysics.swmed.edu/MBR/software.html) [27]. Standard equations and protocols described in Salvay and Ebel [28] were used to derive the micelle sedimentation coefficient at infinite dilution, s_0. We used the Svedberg equation to derive from s, micelle molar masses, M_{mic}, from which were derived aggregation numbers, N_{agg}, using the information on the calculated surfactant molar masses and partial specific volumes reported in Table 2, and estimates on the hydrodynamic diameters from DLS.

2.2.5. SAXS experiments

They were conducted on the BM29 beamline at the European Synchrotron Radiation Facility (Grenoble, France). The data were recorded for $0.004<Q<0.5$ Å^{-1} ($Q=(4\pi/\lambda)\sin\Theta$ is the modulus of the scattering vector, with 2Θ being the scattering angle, and λ the wavelength), using a two-dimensional 1 M Pilatus (Pilatus3 2 M or F_6H_3SB) detector, at 20 °C, with a monochromatic X-ray beam with $\lambda = 0.9919$ Å and a sample to detector distance of 2.864 m. Measurements were typically performed with 80 μL sample, in a quartz capillary, with a continuous flow and 20 acquisitions with 0.5 s irradiation per acquisition recorded for the samples and the water solvent. Data reduction was performed using the automated standard beamline software (BSxCuBE) [29], and data processing, including the elimination of data suffering from radiation damage, averaging, buffer subtraction, Guinier and P(r) plots, using PRIMUS of the software suite ATSAS V8.2.4 [30]. Absolute scales were obtained using the scattering of water. Samples were prepared in water, from dilution of 50 mM stock solutions. For F_6H_3SB, incomplete solubilization was observed, the nominal concentration of 5.6 mM is thus overestimated in an unknown extent. F_5H_5SB, F_6H_3AO, and F_5H_5AO were measured at 6 to 10 different concentrations, respectively, between 2 and 3 mM, and 50 mM. The radius of gyration, R_g, and forward intensity $I(Q = 0)$, were obtained from the linear extrapolation of the Guinier plot, from the smallest Q and in the range $R_gQ<1.3$. From $I(Q = 0)$, given the sample concentration is known, the mean molar mass can be derived. For the investigated samples, we suspect that large, hidden in view of the Q-range, aggregates contribute to decrease the effective concentration of measurable particles. Even for the relatively homogeneous F_5H_5SB, derived N_{agg} are smaller (22 at 5 mM, and 38 at 50 mM), than that estimated from AUC. We thus consider that the analysis in terms of molar mass, thus N_{agg} is inappropriate.

2.2.6. Negative stain electron microscopy

Negatively stained samples were prepared by spreading 5 μl of the dispersion onto a Cu grid coated with a Formvar-film (PLANO,

Wetzlar, Germany). After 1 min, excess liquid was blotted off with filter paper and 5 µl of 1% aqueous uranyl acetate solution were placed onto the grid and drained off after 1 min. Specimens were air-dried and examined in an EM 900 transmission electron microscope (Carl Zeiss Microscopy GmbH, Oberkochen, Germany). Micrographs were taken with a SSCCD SM-1k-120 camera (TRS, Moorenweis, Germany).

2.2.7. Solubilization kinetics

For determining the kinetics of vesicle solubilization, POPC LUVs were prepared by dissolving POPC in powder form in phosphate buffer (10 mM NaH_2PO_4/Na_2HPO_4 in total and 150 mM NaCl at pH 7.4) and shaking for several minutes. The suspension was extruded using a LiposoFast extruder (Avestin, Mannheim, Germany) with at least 35 repeats through two stacked polycarbonate membranes having a pore diameter of 100 nm (Avestin). These LUVs were mixed with the detergents in a 3 × 3 mm cuvette. Immediately after mixing, the measurement was started on a Nano Zetasizer S90 (Malvern), optimized for static light scattering measurements.

2.3. Biochemical evaluation

2.3.1. bR purification and assay

Purified purple membrane was solubilized for 40 h at 4 °C with 89 mM Octylthioglucoside (CMC = 9 mM) at a membrane concentration of 1.5 g L^{-1} in 20 mM sodium phosphate buffer (NaH_2PO_4/Na_2HPO_4), pH 6.8. Samples were diluted to reach a final Octylthioglucoside concentration of 15 mM, supplemented with 2 mM of the surfactant to be tested, and incubated 15 min prior to being loaded onto a 10–30% (w/w) sucrose gradient containing 20 mM sodium phosphate buffer pH 6.8 and either DDM as a control, or the surfactant to be tested, at the following concentrations: DDM: 2.18 mM; F_6H_3SB: 4.23 mM; F_5H_5SB: 4.5 mM; SB-12: 4.84 mM; F_5H_5AO: 3.4, and 6.4 mM; LDAO: 4.2 mM, corresponding to CMC + 2 mM, except F_5H_5AO: 6.4 mM (CMC+ 5 mM). Gradients were centrifuged for 5 h at 55,000 rpm (200,000g) in the TLS55 rotor of a TL100 ultracentrifuge (Beckman). Bands containing the colored protein were collected with a syringe, and protein samples were kept at 4 °C in the dark for UV–visible spectrophotometry.

2.3.2. BmrA, SpNox

Overexpression and purification of BmrA at ≈ 1.5 mg/mL were done according to Mathieu et al. [31] with minor modifications: Solubilization in 1% DDM; elution from NiNTA and dialysis in 50 mM Hepes-KOH pH 8, 10%, glycerol 100 mM NaCl with 0.1% (2 mM) DDM. SpNOX was overexpressed and purified at 1 mg/mL in 50 mM Tris pH 7, 300 mM NaCl, 10 µM FAD with 0.3 mM DDM, as previously described [32], except solubilization was done in 7.4 mM DDM. A final 6-times concentration step was done by ultrafiltration with 50 kDa cut off (Amicon® Ultra-4 Centrifugal Filter Units). SpNOX and BmrA assays were done by dilution as described in Wehbie et al., (See the supporting information section of reference [20]) at the desired final surfactant concentration, and DDM final concentration being under the CMC.

3. Results and discussion

3.1. Synthesis

We used two fluorinated chains for the formation of the zwitterionic detergents, a perfluorohexyl chain (C_6F_{13}) and a perfluoropentyl chain (C_5F_{11}). The use of 5 and 6 fluorinated carbon chains usually yields surfactants whose CMC is in the millimolar range (0.1–5 mM) while allowing sufficient water solubility. Our choice was guided by previous works where similar sulfobetaine [33] and aminoxide [34] fluorinated surfactants were synthesized and whose CMC were 0.31 and 0.16 mM, respectively. We based our synthetic strategy on the radical insertion of iodoperfluoroalkanes into olefins so as to obtain a hydrogenated spacer between the fluorinated chain and the polar head group. In a previous work, we have shown that for the given perfluoropentyl chain, both propyl and pentyl hydrogenated spacer arm led to optimized maltoside fluorinated detergents namely F_5OM and F_5DM with good water solubility, millimolar CMC and close-to-native environment for bR while the commercially perfluorohexyl derivative with an ethyl spacer F_6OM led to rapid aggregation of bR [20]. Therefore, we used the allyl and the penten-1-yl groups from the commercially available allylamine and pent-4-en-1-ol, respectively, onto which the iodoperfluoroalkanes $C_6F_{13}I$ and $C_5F_{11}I$ were introduced. To this end, we developed two synthetic routes (Scheme 1). Performing in parallel the two synthetic routes allowed us to compare them and define which one was the most efficient both in term of overall yield and number of steps. The formation of both sulfobetaine and amine oxide polar head groups can be easily achieved, respectively, through the functionalization of a dimethyl amino group by 1,3-propanesultone and through the direct oxidation of the dimethyl amino group.

The two derivatives containing six fluorinated carbons and a linker comprising three hydrogenated carbons, called F_6H_3AO and F_6H_3SB, were prepared from commercial allylamine following the first retrosynthetic strategy (Scheme 1, route (A)). The two other derivatives F_5H_5AO and F_5H_5SB were prepared following the second retrosynthetic strategy (Scheme 1, route (B)).

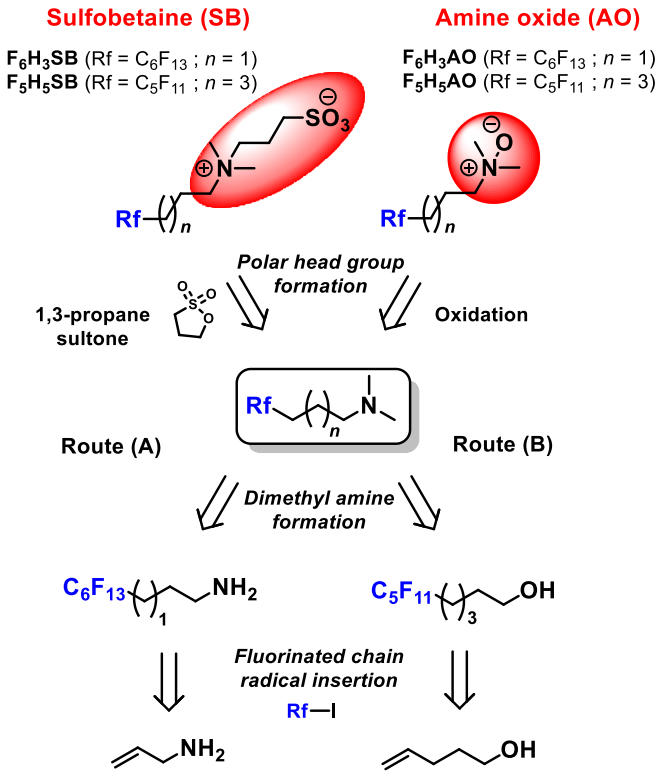

Scheme 1. Retrosynthetic pathways for the sulfobetaine and the amine oxide derivatives. (Left) Route A from allylamine. (Right) Route B from pent-4-en-1-ol. Rf is C_5F_{11} or C_6F_{13}.

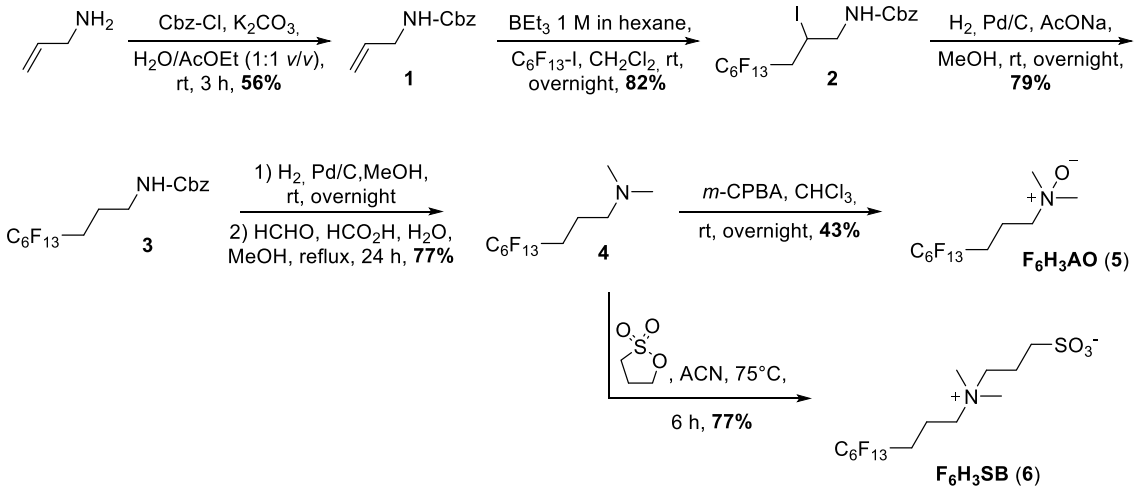

Scheme 2. Synthetic route leading to the derivatives F_6H_3AO and F_6H_3SB.

3.1.1. *Synthesis of F_6H_3AO and F_6H_3SB (Scheme 2)*

The amino function of allylamine was first protected with a carboxybenzyl group according to the procedure described by Olson et al. [22] to obtain **1** in 56% yield. The fluorinated chain was then introduced on the allyl moiety by radical addition of perfluorohexyliodide with the use of triethylborane in the presence of oxygen as described by Takeyama and co-workers [35]. Under these mild conditions, compound **2** was obtained in 82% yield after purification by flash chromatography. Reduction of the C-I bond was achieved by catalytic hydrogenation under alkaline conditions in the presence of Pd/C and led to compound **3** in 79% yield. Under these basic conditions, the carboxybenzyl protecting group remained intact, as reported in the literature [36]. Compound **3** was then submitted to a catalytic hydrogenation to deprotect the amine function followed by an Eschweiler–Clarke reaction [37] to obtain the dimethylamine derivative **4** in 77% yield. Finally, **4** was oxidized with *m*-chloroperoxybenzoic (*m*-CPBA) acid to give the amine oxide derivative F_6H_3AO (**5**) in 43% yield after purification by recrystallization. The reaction of dimethylamine **4** with propane-1,3-sultone yielded the sulfobetaine derivative F_6H_3SB (**6**) as a white precipitate in 77% yield. Of note, F_6H_3SB had already been synthesized following another synthetic route in two steps starting from 3-(perfluorohexyl)propyl iodide [23]. Despite being 3 steps longer, our strategy uses a fluorinated starting material that is significantly cheaper, which makes the scale-up of the synthesis more conceivable.

3.1.2. *Synthesis of F_5H_5AO and F_5H_5SB (Scheme 3)*

This synthetic route involved first the introduction of the fluorinated chain by the radical addition of perfluoropentyliodide on pent-4-enol with the use of triethylborane in the presence of oxygen to obtain **7** in 88% yield. Compound **7** was then submitted to a catalytic hydrogenation in the presence of Pd/C and AcONa to give **8** in 94% yield. The mesyl derivative **9** was prepared in 85% yield by treating the alcohol **8** and methanesulfonyl chloride in the presence of triethylamine. A nucleophilic substitution of **9** with dimethylamine gave derivative **10** in 53% yield after purification by flash chromatography. Compound **10** was oxidized with a solution of 30% wt. H_2O_2 in H_2O to give the amine oxide derivative F_5H_5AO (**11**) in a good yield of 88%. We also tried to obtain F_5H_5AO by oxidation of **10** with *m*-chloroperoxybenzoic acid with no success. Finally, the reaction of dimethylamine **10** with propane-1,3-sultone yielded the sulfobetaine derivative F_5H_5SB (**12**) as a white precipitate in 78% yield.

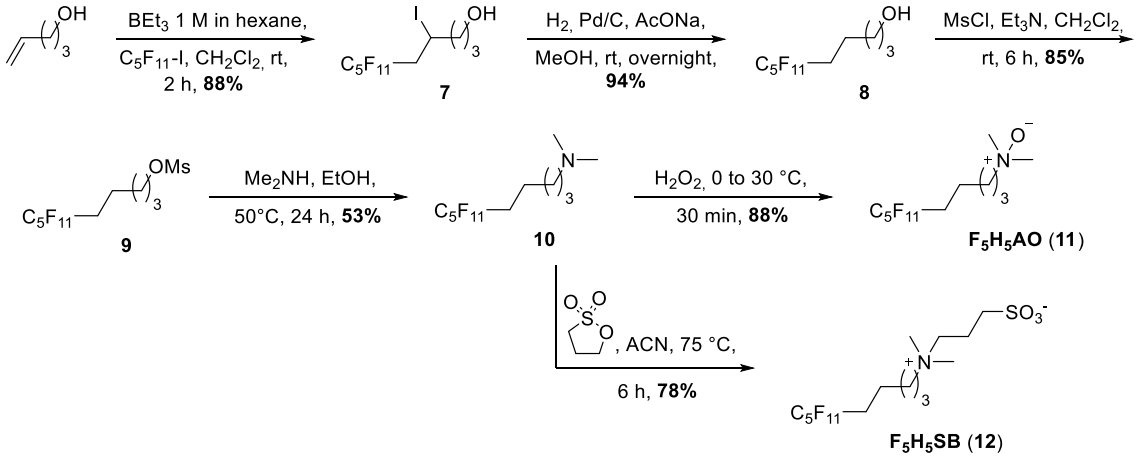

Scheme 3. Synthetic route leading to the derivatives F_5H_5AO and F_5H_5SB.

When comparing the two synthetic routes, route B is more efficient with overall yields of 29% and 33% for F_5H_5AO and F_5H_5SB, respectively, whereas those for F_6H_3AO and F_6H_3SB are 12% and 22%, respectively. These two strategies based on radical addition of iodoperfluoroalkanes onto olefins pave the way to the preparation of other analogs in which the length of the hydrogenated spacer could be varied from 3 to several carbon atoms.

3.2. Colloidal properties

3.2.1. Micellization

Micellization of the four new compounds was characterized by means of ITC and SFT, from which we derived micellar parameters (Table 1, Fig. 2A and B, and Fig. S2). The contributions to the micellization of the F_5H_5 and F_6H_3 hydrophobic chains were similar, as CF_2 groups are known to exhibit about 1.5-fold higher hydrophobicity compared with CH_2 groups [38]. Thus, for a given polar head group, the two derivatives showed similar CMC values. By contrast, for a given chain, the aminoxide detergents exhibited two-fold lower CMCs. The same relative difference in CMC values was also observed for the two fully hydrogenated dodecyl analogs SB-12 and LDAO, whose CMCs were found to be 3.6 mM and 1.7 mM, respectively (see Table S1 for details).

The changes in Gibbs energy $\Delta G_S^{m/aq,\circ}$, enthalpy $\Delta H_S^{m/aq,\circ}$, and entropy $-T\Delta S_S^{m/aq,\circ}$, accompanying the transfer of detergent monomers from the aqueous solution into micelles are also summarized in Table 1. These data showed that micellization was almost exclusively driven by entropy, with enthalpy making only a minor contribution. Yet, the enthalpic contribution to micelle formation was more pronounced in the case of the aminoxide derivatives than for the sulfobetaine derivatives. SFT data were used to construct Gibbs adsorption isotherms (data not shown) to determine the surface excess concentration at surface saturation, Γ_{max}, and the area occupied per detergent molecule at the air/water interface, A_{min}. The values observed for F_6H_3SB and F_5H_5SB (3.20×10^{-12} mol/mm^2) and for F_6H_3AO and F_5H_5AO (4.40×10^{-12} mol/mm^2) indicate a tighter packing at the air/water interface of the amine oxide derivatives and, thus, result in lower occupied areas, with 38 Å^2 for the amine oxide derivatives and 51 Å^2 for the sulfobetaine derivatives. For the hydrogenated analogs SB-12 and LDAO, we measured larger A_{min} values of 63 Å^2 and 46 Å^2 (Table S1), respectively, suggesting that fluorinated chains favor tighter packing at the air/water interface.

Table 2
DLS, AUC, and SAXS data of F_6H_3AO, F_5H_5AO, F_6H_3SB, and F_5H_5SB.

		F_6H_3SB	F_5H_5SB	F_6H_3AO	F_5H_5AO
DLS	d_H (nm) – Int.[a]	11.1	6.2	10.0	6.7
	d_H (nm) – Vol.[a]	7.8	5.7	10.7	5.6
	d_0 (nm) – Vol.	n.d.	6.2	7.0	7.3
AUC	$\bar{\nu}$ (mL/g)[b]	0.562	0.611	0.514	0.573
	s_0 (S)[c]	6.8 ± 0.2	4.6 ± 0.2	n.d.	7.1 ± 0.2
	s (S)[c]	7.3 ± 0.2	5.0 ± 0.2	35 ± 5	7.4 ± 0.2
	k'_s (mL/g)[d]	29	29	n.d.	16
	M (kDa)[e]	77 ± 9	44 ± 5	450 ± 29	59 ± 8
	N_{agg}[e]	143 ± 16	87 ± 10	1067 ± 69	148 ± 20
	f/f_{min}[e]	1.56 ± 0.14	1.37 ± 0.16	1.22 ± 0.14	1.26 ± 0.15
SAXS	R_g (nm)[f]	2.7 ± 0.05	2.1 ± 0.2	30 ± 1	7.2 ± 1
	D_{max} (nm)[f]	12 ± 1	7.5 ± 0.1	250 ± 10	36 ± 5

[a] Hydrodynamic diameters by dynamic light scattering measured in water at 3.6 × CMC for F_6H_3SB (~9.7 mM) and at 10 × CMC for F_5H_5SB (~24.5 mM), F_6H_3AO (~12.9 mM) and F_5H_5AO (~9.9 mM) and calculated at infinite dilution (d_0). Data are averages of at least three experiments made of ten runs.
[b] Partial specific volume calculated from chemical composition.
[c] Sedimentation coefficient at infinite dilution (s_0), or linearly interpolated from experimental data at CMC + 5 mM, in water at 20 °C.
[d] Concentration dependence factor k's from linear fits.
[e] Molar mass, aggregation number, and frictional ratio obtained from s and D_H. Error is estimated at 10%.
[f] Radius of gyration from Guinier analysis and maximum diameter from P(r) analysis at ≈ 5 mM.

3.2.2. Size and shape of micelles

Next, we investigated the self-assembly properties of the fluorinated surfactants in pure water using DLS. The data are given in Table 2. At 10 × CMC, volume-weighted particle size distributions revealed unimodal distributions of small micelles with hydrodynamic diameters, d_H, ranging from ~6 nm for F_5H_5AO and F_5H_5SB to ~11 nm for F_6H_3AO (Fig. 2C and D). Because of its lower water solubility, F_6H_3SB was observed at 3.6 × CMC showing unimodal distributions of micelles with a diameter of ~8 nm. By comparison, slightly smaller micelles were observed for hydrogenated LDAO and SB-12 with hydrodynamic diameters of 3.2 nm and 4.3 nm, respectively (Fig. 2C and D). Upon varying the concentration from 6 to 16 × CMC, no major differences in the volume-weighted distributions were observed (Fig. S3). At 10 × CMC, intensity-weighed particle size distributions revealed multimodal distributions for the four compounds, with larger particles that accounted only for a small fraction of the total material present in the samples (Fig. S4).

Table 1
Micellization properties of sulfobetaine and amine oxide derivatives.

Detergent		F_6H_3SB (6)	F_5H_5SB (12)	F_6H_3AO (5)	F_5H_5AO (11)
Molecular Weight g/mol		527.34	505.39	421.20	399.25
ITC[a]	CMC (mM)	2.23 ± 0.01	2.43 ± 0.02	1.31 ± 0.02	1.40 ± 0.03
	$-T\Delta S^\circ_{mic}$ (kJ/mol)[b]	−26.88 ± 0.08	−26.85 ± 0.11	−31.60 ± 0.45	−34.07 ± 0.92
	ΔH°_{mic} (kJ/mol)[c]	1.79 ± 0.06	1.97 ± 0.09	5.20 ± 0.44	7.83 ± 0.87
	ΔG°_{mic} (kJ/mol)[d]	−25.09 ± 0.01	−24.88 ± 0.02	−26.41 ± 0.04	−26.25 ± 0.05
	K^{mic} (× 10^4)	2.49 ± 0.01	2.29 ± 0.02	4.24 ± 0.06	3.97 ± 0.08
ST[a]	CMC (mM)	2.67 ± 0.05	2.52 ± 0.08	1.22 ± 0.09	1.04 ± 0.00
	ΔG°_{mic} (kJ/mol)[d]	−24.6 ± 0.05	−24.8 ± 0.08	−26.6 ± 0.2	−27.0 ± 0.07
	γCMC (mN/m)[e]	25.5 ± 0.9	25.5 ± 0.9	19.2 ± 0.7	18.5 ± 0.2
	Γ_{max} (10^{-12} mol/mm^2)	3.20 ± 0.11	3.20 ± 0.04	4.40 ± 0.30	4.30 ± 0.01
	A_{min} (Å^2)[f]	51.2 ± 1.7	51.5 ± 1.7	37.7 ± 2.8	38.4 ± 0.08

[a] Data are averages of at least two experiments. ± indicates 95% confidence interval boundaries from a nonlinear least-squares fit for ITC. ± indicates standard errors from at least two experiments for SFT.
[b] Entropic contribution to micelle formation.
[c] Enthalpic contribution to micelle formation.
[d] Gibbs energy of micellization.
[e] Surface tension attained at the CMC.
[f] Surface excess (Γ_{max}) and surface area per molecule (Å^2) were estimated from the slope of the surface tension curve.

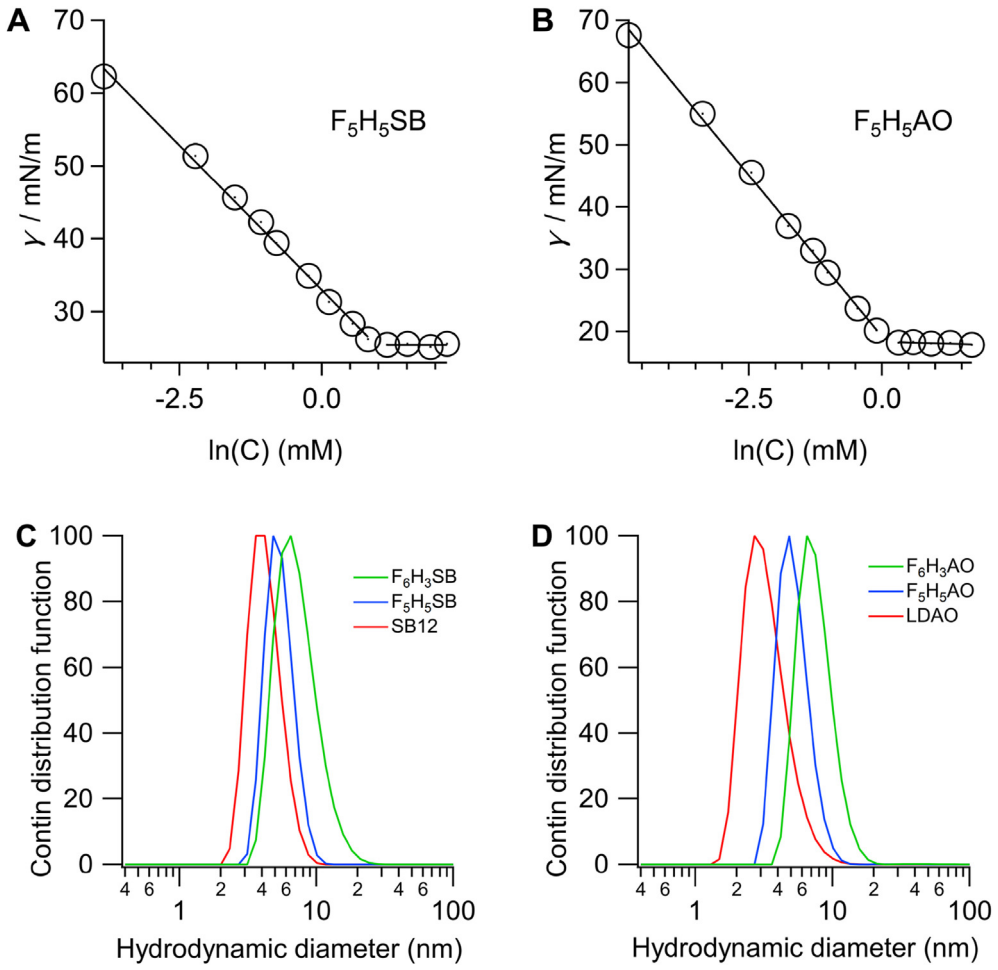

Fig. 2. Surface tension versus concentration for (A) F_5H_5SB and (B) F_5H_5AO. Solid lines represent linear fits to experimental data points, where the intersection corresponds to the CMC. Volume-weighted particle size distributions in water of (C) SB-12 and F_5H_5SB at 10 × CMC (36 and 24.3 mM, respectively) and F_6H_3SB at 3.6 × CMC (8 mM) and of (D) LDAO, F_6H_3AO, and F_5H_5AO at 10 × CMC (17, 13.1, and 14 mM, respectively).

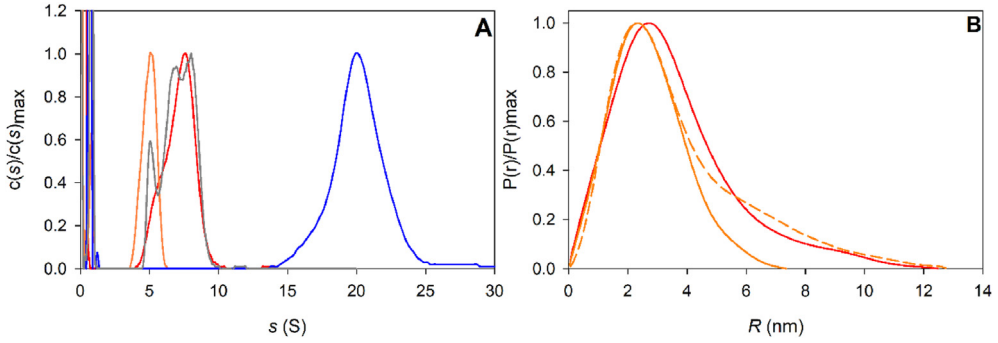

Fig. 3. (A) Sedimentation coefficient distributions, c(*s*), of F_6H_3SB (red), F_5H_5SB (orange), F_6H_3AO (blue), and F_5H_5AO (grey) at 8, 8, 3.7, and 5 mM, respectively, in water and at 20 °C. (B) SAXS results summarized as P(r) of F_6H_3SB at 6.25 mM (continuous red line), and F_5H_5SB (orange), at 5 (continuous line) and 50 mM (dash line).

More information on the size and shape of the micelles was obtained from AUC. Out of the four surfactants, three revealed relatively well-defined sedimentation coefficient distributions (Fig. 3A, Figs. S5 and S6). F_5H_5SB revealed the smallest *s*-value (s_0 = 4.2 S), while F_6H_3SB and F_5H_5AO behaved similarly with s_0 = 6.8 and 7.1 S, respectively. For these three surfactants, modest attractive interactions among the micelles are evidenced from concentration dependence. F_6H_3AO exhibited a different size distribution with large *s*-values (18–36 S) and nonlinear concentration dependence of the *s*-value (Fig. S7). Molar masses (*M*) and aggregation numbers (N_{agg}) of the micelles were derived combining d_H from DLS (Table 2, second line) and *s*-values obtained from AUC 5 mM above the respective CMC. The micelles of F_5H_5SB were found to be the smallest ($N_{agg} \approx 90$), followed by those of F_6H_3SB and F_5H_5AO ($N_{agg} \approx 150$). By contrast, F_6H_3AO formed very large micelles ($N_{agg} \approx 1000$). The frictional ratios of 1.4 ± 0.2 would

indicate, in view of the uncertainties, moderately anisotropic or nearly globular micellar shapes (Table 2), which is reasonable for the small assemblies, but questionable for the large ones F_6H_3AO.

The characterization of the micelles was completed by SAXS (Table 2). The two sulfobetaine derivatives formed small micelles. At 6.25 mM nominal concentration, F_6H_3SB is composed essentially of small assemblies (Table 2, Fig. 3B). F_5H_5SB in the mM range presents the smallest assemblies of the four derivatives with R_g of 2.1 nm, D_{max} of 2.1 nm, with a rather symmetrical pair distribution curve suggesting globular shape. The micelle size R_g and D_{max} very slightly increase above ≈15 mM, reaching R_g = 3.0 and D_{max} = 13 nm at 50 mM (Fig. 3B, Fig. S8). Traces of very large aggregates were detected at very small $Q < 0.01$ nm^{-1}) (Figs. S9 and S10). For the two aminoxide derivatives, the shape of the scattering curves and the non-linear Guinier plots indicate micelle heterogeneity (Figs. S9 and S10). For F_6H_3AO at 5.7 mM, the R_g of 30 nm and D_{max} at 250 nm indicate rather large objects, whose size increased with concentration (Fig. S8). Above 15 mM, a break in the Guinier plot and the pair distribution functions suggest two populations of very large (D_{max} ≈ 300 nm) and small species (R_g = 2.2 nm, D_{max} = 6.4 nm at 50 mM). For F_5H_5AO, from 5 to 50 mM, the R_g increases from 7 to 14 nm, respectively, and D_{max} from 36 to 70 nm, respectively, indicating the formation of moderately large oligomers of larger size when increasing concentration (Figs. S8–S11).

Finally, transmission electron microscopy (TEM) experiments were performed. Sample concentration was slightly above the CMC, which is still far above the usual concentration to allow quantitative observation. Therefore, only qualitative observations can be made from these experiments. Fig. 4 shows representative EM micrographs of negatively stained samples of the four fluorinated surfactants. Due to the high concentration of detergent many aggregates were observed on the grid, which hinders good visualization of the individual aggregate shape and an accurate determination of the size. Nonetheless, the particles observed by TEM were round-shaped and exhibited diameters of 15–75 nm for F_6H_3SB, 5–25 nm for F_5H_5SB, 10–18 nm for F_6H_3AO and 5–30 nm for F_5H_5AO.

Taken together, the four structural techniques used here indicated that F_5H_5SB formed the smallest micelles within the series of new detergents. The size of the micelles increased only slightly with concentration. F_6H_3SB, investigated below 10 mM because of its low solubility, formed somewhat larger micelles F_5H_5SB did. F_5H_5AO micelles appeared similar in size to those of F_5H_5SB both by DLS and TEM and slightly larger according to AUC, and polydisperse by SAXS. Finally, F_6H_3AO assemblies were also heterogeneous in size, forming both small, spherical micelles as well as very large aggregates.

3.2.3. Vesicles solubilization

To test the ability of the new fluorinated detergents to solubilize lipid bilayers, we monitored the solubilization of large unilamellar vesicles (LUVs) made of 1-palmitoyl-2-oleyl-*sn*-glycero-3-phosphocholine (POPC) by light scattering measurements [19].

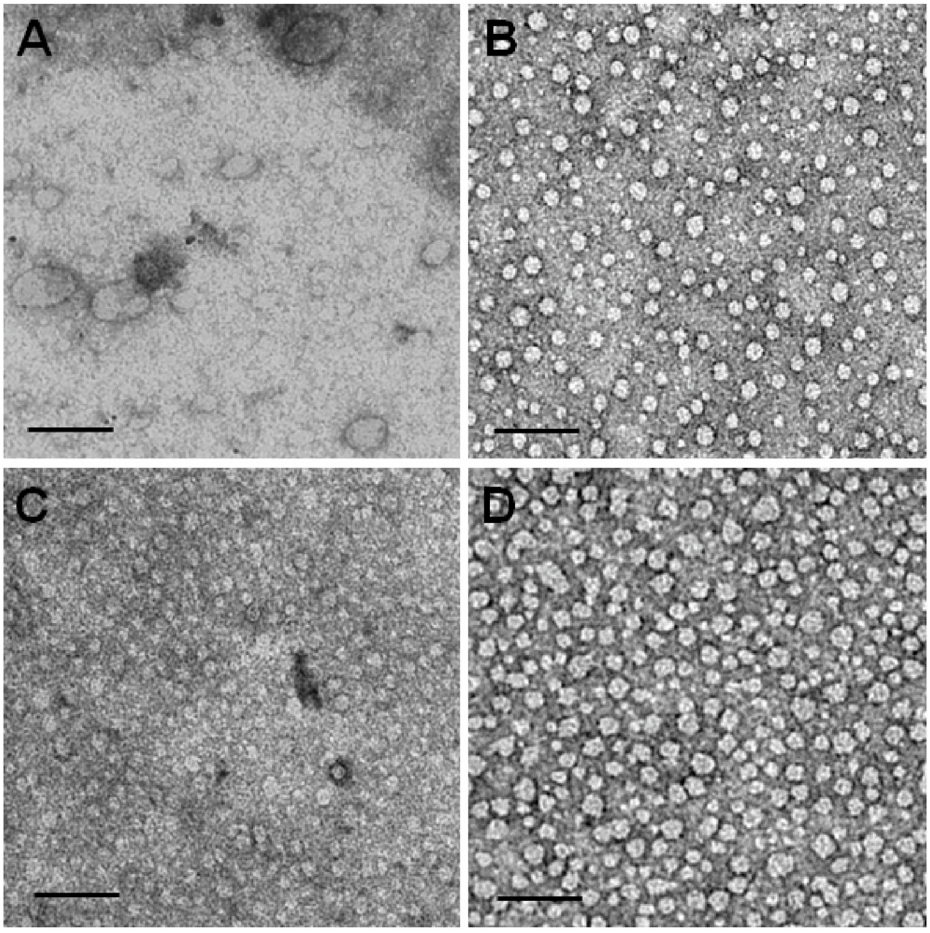

Fig. 4. Negative-stain TEM of round-shaped detergent assemblies: (A) F_6H_3SB, (B) F_5H_5SB, (C) F_6H_3AO and (D) F_5H_5AO at 2.7 mM, 2.4 mM, 1.8 mM, and 1.4 mM, respectively. Scale bar: 100 nm.

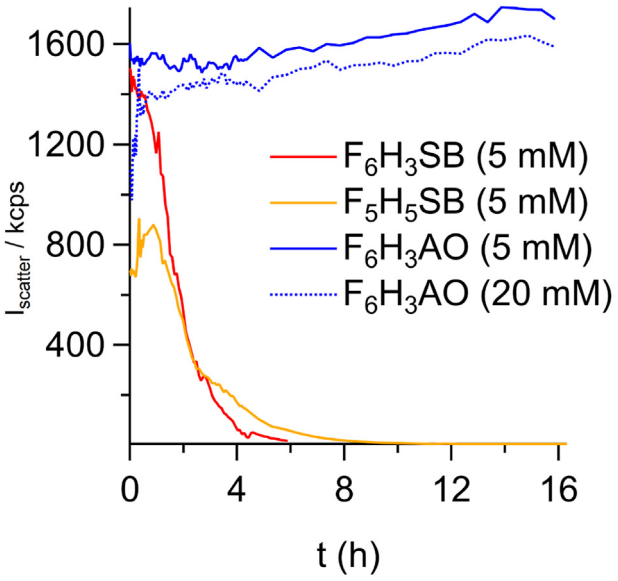

Fig. 5. Kinetics of vesicle solubilization. 0.3 mM POPC LUVs solubilized by 5 mM F_5H_5SB (red), 5 mM F_6H_3SB (green), and either 5 mM or 20 mM F_6H_3AO (blue) at 50 °C as monitored in terms of the light scattering intensity recorded at an angle of 90°.

Even at an elevated temperature of 50 °C, solubilization of 0.3 mM POPC LUVs required ~4 h for F_6H_3SB and ~8 h for F_5H_5SB when each detergent was present at 5 mM above its respective CMC (Fig. 5). These slow solubilization processes indicate that these two compounds exhibit moderate detergency towards artificial membranes. The nature of the mixed lipid/detergent assemblies formed by the solubilization of LUVs was investigated by negative-stain TEM. While F_5H_5SB formed spherical mixed micelles upon mixing with lipids (not shown), F_6H_3SB gave rise to discoidal assemblies (Fig. S12), which are often referred to as nanodiscs. Such nanodiscs typically result from nanoscale demixing of the lipid and the solubilizing detergent, resulting in a planar lipid-bilayer patch surrounded by a detergent belt. The observation of nanodiscs in F_6H_3SB/POPC mixtures is reminiscent of recent findings made using (fluorinated) diglucose detergents [39]. Regarding the two amine oxide derivatives, opposing solubilization behaviors were observed for the two different chains. While F_6H_3AO failed to solubilize POPC even when its concentration was raised to 20 mM above its CMC (Fig. 5), F_5H_5AO caused solubilization of LUVs even at room temperature within a few seconds and thus, was not measurable (data not shown). The difference observed between the two amine oxide compound is difficult to explain based on their similar CMC and chemical composition. Although speculative, this might come the difference of their self-aggregation properties with the F_6H_3AO forming two populations of small and large aggregates that inhibit the solubilization process.

3.3. Biochemical evaluation

3.3.1. Bacteriorhodopsin homogeneity and stability

To assess the usefulness of the new detergents for membrane-protein applications, we investigated the homogeneity and stability over time of bacteriorhodopsin (bR). This model membrane protein is composed of seven transmembrane α-helices and binds a covalent cofactor, a retinal molecule that confers purple color to the protein. We used sucrose gradients as a convenient means to perform both detergent exchange and to evaluate the colloidal homogeneity of the protein/detergent complex (Fig. 6 and S13)

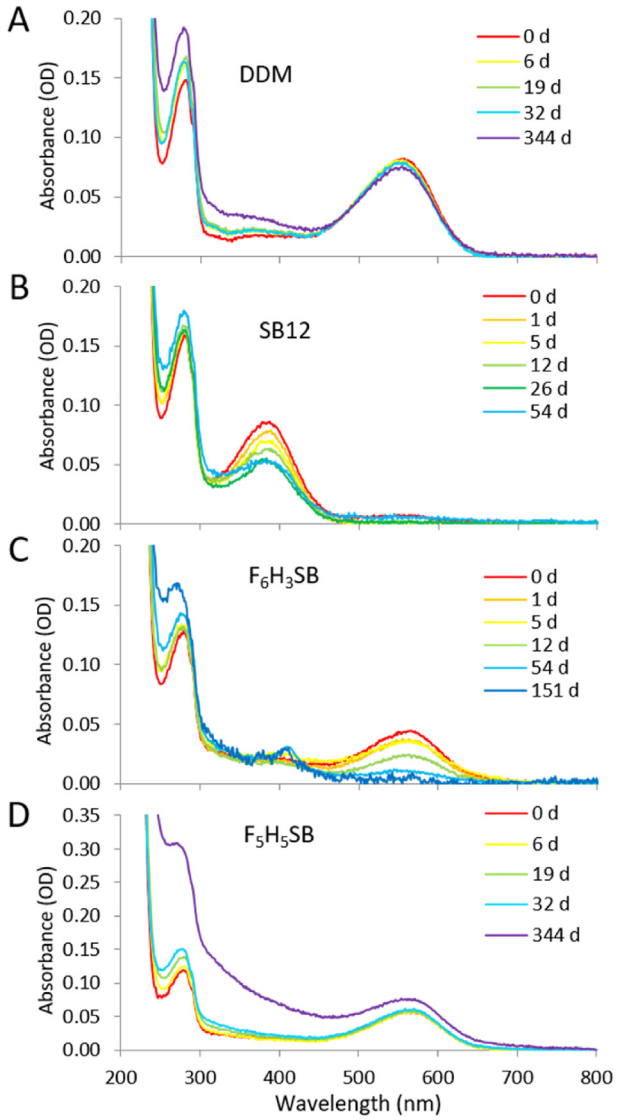

Fig. 6. Spectral time course of bR transferred in (A) DDM, (B) SB-12, (C) F_6H_3SB and (D) F_5H_5SB at CMC + 2 mM. Detergent exchange was performed by centrifugation on sucrose gradient. Samples were incubated at 4 °C in the dark and UV–visible spectra were recorded at the indicated time (given in days (d)). Time 0 corresponds to the sample collected from the gradient right after centrifugation.

[15]. The detergent concentration was fixed at 2 mM above its CMC. After centrifugation for 5 h, the protein in DDM, SB-12, and LDAO migrated as a thin pink band in the first third of the gradient (Fig. S14). Whereas bR in DDM revealed its typical spectrum for a folded monomer in detergent (λ_{max} ~554 nm), which remained stable over time, bR in SB-12 showed a spectrum with λ_{max} at ~390 nm, indicating a denatured protein (Fig. 6); bR spectrum in LDAO indicates scattering by large aggregates and displays a λ_{max} at ~390 nm (Fig. S13). Thus, in the two zwitterionic hydrogenated detergents, bR was found not stable at all.

When transferred into F_6H_3SB or F_5H_5SB, the protein migrated deeper into the gradients, as expected due to the higher density of the surfactants (Fig. S14). More importantly, bR revealed spectra characterized by λ_{max} at ~565 nm in F_6H_3SB and ~570 nm in F_5H_5SB (Fig. 6). A shift in λ_{max} when bR is transferred into fluorinated surfactants has already been reported [15]. In F_6H_3SB, bR fully denatured after a month, whereas in F_5H_5SB, the spectrum remained unchanged upon storage of the sample in the dark for one month

(Fig. 6). After one year, λ_{max} remains unchanged, however protein aggregated, as revealed by scattering in the spectrum, as was the case in DDM. These findings demonstrated that bR is significantly more stable in these two fluorinated detergents than in their hydrogenated counterparts. By contrast, when transferred into F_6H_3AO or F_5H_5AO, the protein was recovered in the pellet of the gradient, indicating the presence of larger aggregates (Fig. S14). The protein in F_5H_5AO was resuspended, and showed a spectrum indicating light scattering, as expected from resuspending a pellet, with a λ_{max} at ~570 nm (Fig. S13). The protein bleached and was completely white after 150 days. To check whether protein aggregation in F_5H_5AO was due to a lack of detergent, we performed a gradient at 5 mM above the CMC. Still, bR aggregated regardless of the surfactant concentration (Fig. S13). In F_5OM or F_5DM, two fluorinated maltose analogs of DDM, λ_{max} rapidly shifted to ~575 nm and remained unchanged for one year; the absence of absorbance at 390 nm reflecting the absence of protein denaturation. This indicates the protein is more stable in the two maltose derivative than in F_6H_3SB. In F_6OM the commercially available fluorinated analogue of DDM, bR was not soluble and aggregated during surfactant exchange.

3.3.2. Enzymatic activity in fluorinated surfactants

We next investigated the enzymatic activity of BmrA a bacterial multidrug ABC transporter homologue of mammalian P-gp [40]. BmrA transports multiple drugs having no obvious chemical relationship outside the bacterium, with the driving force of ATP hydrolysis, and has been shown to adopt different conformations during its catalytic cycle [41]. Here, BmrA activity was measured spectroscopically by following the absorbance at 340 nm as a measure of NADH oxidation, which correlates with ATP hydrolysis. BmrA was extracted by DDM before detergent exchange was done by dilution, which resulted in a final DDM concentration below its CMC. Activity assays in DDM at CMC + 0.1, 1, 2 and 5 mM, showed that the activity was the largest and standard deviations the smallest at CMC + 2 mM (Table S2). Thus, the activity was expressed relative to that in DDM alone at a detergent concentration of CMC + 2 mM. We thus found that F_6H_3SB outperformed DDM at lower concentration, CMC +0.5 mM being the condition with the largest specific activity (Fig. 7). The largest specific activity in F_6H_3SB is in line with the previous work where we demonstrated that the ATPase activity of BmrA in the fluorinated detergent FLAC6 was ~2.5 times higher than in DDM [21]. BmrA in F_5H_5SB showed significantly lower enzymatic activity, although it remained in the same range as that afforded in the fully hydrogenated detergent SB-12. F_6H_3AO preserved activity of BmrA to almost the same extent as DDM at quite low concentrations (0.2–0.5 mM), whereas the activity of BmrA in F_5H_5AO was close to that in F_5H_5SB. The hydrogenated LAPAO derivative failed to preserve any BmrA activity. For a given polar head, this demonstrates the superiority of the new fluorinated derivatives over their hydrogenated counterpart to preserve the enzymatic activity of BmrA. As regards the effect of the polar head, the three fluorinated maltose derivatives F_5OM, F_5DM and F_6OM induced a drop of 40–90% in the specific activity of BmrA compared to DDM [20]. In this work we demonstrate the two zwitterionic F_6H_3-SB and F_6H_3AO preserve more protein activity than their maltose analogs despite the presence of a more denaturing zwitterionic polar head.

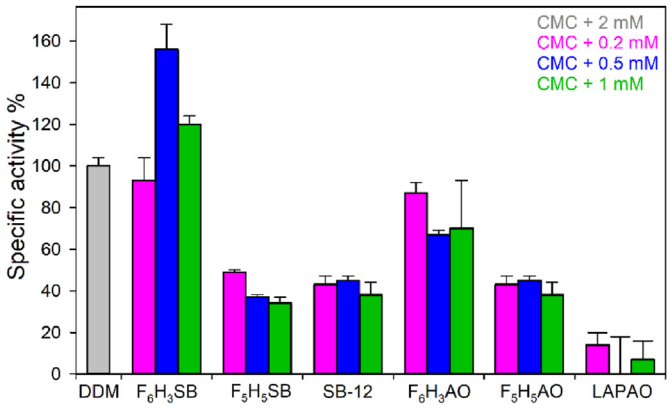

Fig. 7. Specific Activity of BmrA at CMC + 0.2 mM (pink), CMC + 0.5 mM (blue), CMC + 1 mM (green). CMC values are from ITC (Table 1). Standard deviations were determined from triplicate experiments from the same preparation. Specific activity was normalized at 100% for measurement in CMC +2 mM DDM. Surfactant exchange was done by dilution.

We also measured the specific activity of SpNOX, a *Streptococcus pneumoniae* protein [42], an analogue of the eukaryotic NADPH oxidase (Fig. S15). For the sulfobetaine series, the two fluorinated compounds preserved the activity of SpNOX, whereas in SB-12, SpNOXshowed no activity. At CMC + 5 mM, F_5H_5SB or F_6H_3SB, the enzymatic activity was about 70% of that observed in DDM. By contrast, for the aminoxide series, in the hydrogenated LAPAO, SpNOX exhibited 90% activity in a detergent concentration range of 1–5 mM, whereas only the F_6H_3AO preserved SpNOX moderate activity of 30–50%. Compared to the three maltose derivatives [20], the two sulfobetaines preserved SpNOX activity only at the highest concentration (CMC + 5 mM).

Finally, the fluorinated sulfobetaine and dimethylamine oxide detergents were tested as additives in the presence of *n*-dodecylmaltoside (DDM) for the crystallization of AcrB, an efflux pump located in the inner membrane of *Escherichia coli*. These preliminary assays suggest that, when used as additives for the crystallization of AcrB in the presence of DDM, the four compounds could improve control nucleation (See the supplementary data for details) as previously observed for other fluorinated surfactants [43].

4. Conclusion

We have synthesized four zwitterionic fluorinated detergents as analogs of the hydrogenated sulfobetaine SB-12 and the hydrogenated aminoxide LDAO. The synthetic route to the F_5H_5 derivatives is more efficient than that of the F_6H_3 derivatives, but both routes enabled gram-scale synthesis of pure compounds. The hydrophobic contribution of the F_6H_3 chain was comparable to that of the F_5H_5 chain and slightly lower than that of a fully hydrogenated dodecyl chain. These new fluorinated detergents formed small, globular micelles in the millimolar range. F_5H_5AO demonstrated strong detergency, as it solubilized lipid vesicles instantly, whereas the two SB derivatives showed moderate detergency with slow solubilization. The SB derivatives outperform the AO ones in stabilizing bR and in preserving the enzymatic activities of BmrA and SpNOX. Taken together, the fluorinated surfactants with the SB head group are better suited than those carrying an AO head group to preserve membrane-protein activity. Still, fluorination of the alkyl chain increases the stabilizing properties of all four compounds compared with their hydrogenated counterparts. Moreover, while the stabilizing properties were increased by using a fluorinated chain, the solubilizing properties were at least partially retained. Among the four compounds, F_5H_5SB combines many desirable properties for membrane-protein study, that is, high water solubility, a CMC in the millimolar range, decent detergency, and good stabilizing properties for several MPs.

Authors' contribution

Marine Soulié: synthesis, SFT and DLS experiments, original draft; Anais Deletraz: synthesis, and SFT experiments; Moheddine Wehbie: synthesis; Florian Mahler: ITC and lipid solubilization experiments; Ihlam Bouchemal: enzymatic activity and crystallization assays; Aline Le Roy: AUC and SAXS experiments and bR stability assays; Isabelle Petit-Härtlein: SpNOX sample production and enzymatic activity measurements; Sandro Keller: supervision of ITC and lipid solubilization experiments, analysis, assistance in writing; Annette Meister: TEM experiments; Eva Pebay-Peyroula: supervision of crystallization assays, analysis, assistance in writing; Cécile Breyton: supervision of bR stability assays, analysis, assistance in writing; Christine Ebel: supervision of AUC and SAXS experiments as well as enzymatic activity, analysis, assistance in the writing. Grégory Durand: conceptualization of the molecules, supervision of the synthesis, SFT and DLS experiments, analysis, writing.

Declaration of competing interest

The authors declare they have no known financial interests or personal relationship that could have appeared to influence the work reported in this paper.

Acknowledgments

This work was supported by the Agence Nationale de la Recherche (ANR) through grants no. ANR-16-CE92-0001 and by the Deutsche Forschungsgemeinschaft (DFG) through grant no. KE 1478/7-1 and ME 4165/2-1. We acknowledge the financial support of the European Regional Development Fund, the French Government, the "Région Provence Alpes Côte d'Azur", the "Département de Vaucluse" and the "Communauté d'agglomération Grand Avignon" for access to the NMR platform (CPER 3A). This work used the platforms of the Grenoble Instruct-ERIC center (ISBG; UAR 3518 CNRS-CEA-UGA-EMBL) within the Grenoble Partnership for Structural Biology (PSB), supported by FRISBI (ANR-10-INBS-0005-02) and GRAL, financed within the University Grenoble Alpes graduate school (Ecoles Universitaires de Recherche) CBH-EUR-GS (ANR-17-EURE-0003). IBS acknowledges integration into the Interdisciplinary Research Institute of Grenoble (IRIG, CEA). We acknowledge the European Synchrotron Radiation Facility for provision of synchrotron radiation facilities and we thank Petra Pernot and Mark Tully for assistance in using beamline BM29. We thank Dr Emilie Grousson (AU) who participated in the synthesis and Emmi Mikkola (UGA) who participated in the biochemical evaluation.

Appendix A. Supplementary data

Supplementary data to this article can be found online at https://doi.org/10.1016/j.biochi.2022.11.003.

References

[1] J.P. Overington, B. Al-Lazikani, A.L. Hopkins, How many drug targets are there? Nat. Rev. Drug Discov. 5 (2006) 993–996.
[2] G.G. Privé, Detergents for the stabilization and crystallization of membrane proteins, Methods 41 (2007) 388–397.
[3] J.-L. Popot, Amphipols, nanodiscs, and fluorinated surfactants: three nonconventional approaches to studying membrane proteins in aqueous solutions, Annu. Rev. Biochem. 79 (2010) 737–775.
[4] C.-j. Cheng, G.-m. Qu, J.-j. Wei, T. Yu, W. Ding, Thermodynamics of micellization of sulfobetaine surfactants in aqueous solution, J. Surfactants Deterg. 15 (2012) 757–763.
[5] A.P. Gerola, P.F.A. Costa, F. Nome, F. Quina, Micellization and adsorption of zwitterionic surfactants at the air/water interface, Curr. Opin. Colloid Interface Sci. 32 (2017) 48–56.
[6] M. Chevallet, V. Santoni, A. Poinas, D. Rouquié, A. Fuchs, S. Kieffer, S. Kieffer, J. Lunardi, J. Garin, T. Rabilloud, New zwitterionic detergents improve the analysis of membrane proteins by two-dimensional electrophoresis, Electrophoresis 19 (1998) 1901–1909.
[7] S. Luche, V. Santoni, T. Rabilloud, Evaluation of nonionic and zwitterionic detergents as membrane protein solubilizers in two-dimensional electrophoresis, Proteomics 3 (2003) 249–253.
[8] C. Tastet, S. Charmont, M. Chevallet, S. Luche, T. Rabilloud, Structure-efficiency relationships of zwitterionic detergents as protein solubilizers in two-dimensional electrophoresis, Proteomics 3 (2003) 111–121.
[9] A. Blanchard, G. Baffet, H. Wróblewski, Highly selective extraction of spiralin from the Spiroplasma citri cell membrane with alkyl-N-sulfobetaines, Biochimie 67 (1985) 1251–1256.
[10] C. Sardet, A. Tardieu, V. Luzzati, Shape and size of bovine rhodopsin: a small-angle X-ray scattering study of a rhodopsin-detergent complex, J. Mol. Biol. 105 (1976) 383–407.
[11] H. Michel, Three-dimensional crystals of a membrane protein complex: the photosynthetic reaction centre from Rhodopseudomonas viridis, J. Mol. Biol. 158 (1982) 567–572.
[12] M. le Maire, P. Champeil, J.V. Moller, Interaction of membrane proteins and lipids with solubilizing detergents, Biochim. Biophys. Acta 1508 (2000) 86–111.
[13] J. Breibeck, A. Rompel, Successful amphiphiles as the key to crystallization of membrane proteins: bridging theory and practice, Biochim. Biophys. Acta Gen. Subj. 1863 (2019) 437–455.
[14] G. Durand, M. Abla, C. Ebel, C. Breyton, New amphiphiles to handle membrane proteins: "Menage a Trois' between chemistry, physical chemistry, and biochemistry, in: I. Mus-Veteau (Ed.), Membrane Proteins Production for Structural Analysis, Springer New York, Place Published, 2014, pp. 205–251.
[15] C. Breyton, F. Gabel, M. Abla, Y. Pierre, F. Lebaupain, G. Durand, J.-L. Popot, C. Ebel, B. Pucci, Micellar and biochemical properties of (hemi)fluorinated surfactants are controlled by the size of the polar head, Biophys. J. 97 (2009) 1–10.
[16] F. Lebaupain, A.G. Salvay, B. Olivier, G. Durand, A.-S. Fabiano, N. Michel, J.-L. Popot, C. Ebel, C. Breyton, B. Pucci, Lactobionamide surfactants with hydrogenated, perfluorinated or hemifluorinated tails: physical-chemical and biochemical characterization, Langmuir 22 (2006) 8881–8890.
[17] C. Breyton, E. Chabaud, Y. Chaudier, B. Pucci, J.L. Popot, Hemifluorinated surfactants: a non-dissociating environment for handling membrane proteins in aqueous solutions? FEBS (Fed. Eur. Biochem. Soc.) Lett. 564 (2004) 312–318.
[18] G.N.M. Boussambe, P. Guillet, F. Mahler, A. Marconnet, C. Vargas, D. Cornut, M. Soulié, C. Ebel, A.L. Roy, A. Jawhari, F. Bonneté, S. Keller, G. Durand, Fluorinated diglucose detergents for membrane-protein extraction, Methods 147 (2018) 84–94.
[19] E. Frotscher, B. Danielczak, C. Vargas, A. Meister, G. Durand, S. Keller, A fluorinated detergent for membrane-protein applications, Angew. Chem. Int. Ed. 54 (2015) 5069–5073.
[20] M. Wehbie, K.K. Onyia, F. Mahler, A. Le Roy, A. Deletraz, I. Bouchemal, C. Vargas, J.O. Babalola, C. Breyton, C. Ebel, S. Keller, G. Durand, Maltose-based fluorinated surfactants for membrane-protein extraction and stabilization, Langmuir 37 (2021) 2111–2122.
[21] C. Faugier, S. Igonet, D. Cornut, R. Besson, G. Durand, A. Jawhari, Lactobionamide-based fluorinated detergent for functional and structural stabilization of membrane proteins, Methods 180 (2020) 19–26.
[22] C.A. Olson, C.E. Shaner, S.C. Roche, G.M. Ferrence, T.A. Mitchell, Hexahydro-1H-Isoindolinone-Like scaffolds from electronically deactivated and sterically hindered dienes: synthesis in the context- of M-uironolide A, Synthesis 47 (2015) 2756–2766.
[23] R. Kaplánek, O. Paleta, Amphiphilic perfluoroalkylated sulfones and sulfonate betaines, J. Fluor. Chem. 128 (2007) 789–796.
[24] S. Keller, C. Vargas, H. Zhao, G. Piszczek, C.A. Brautigam, P. Schuck, High-precision isothermal titration calorimetry with automated peak-shape analysis, Anal. Chem. 84 (2012) 5066–5073.
[25] S.-C. Tso, F. Mahler, J. Höring, S. Keller, C.A. Brautigam, Fast and Robust quantification of detergent micellization thermodynamics from isothermal titration calorimetry, Anal. Chem. 92 (2020) 1154–1161.
[26] P. Schuck, Size-distribution analysis of macromolecules by sedimentation velocity ultracentrifugation and Lamm equation modeling, Biophys. J. 78 (2000) 1606–1619.
[27] C.A. Brautigam, Chapter five - calculations and publication-quality illustrations for analytical ultracentrifugation data, in: J.L. Cole (Ed.), Methods in Enzymology, Academic Press, Place Published, 2015, pp. 109–133.
[28] A.G. Salvay, C. Ebel, Analytical ultracentrifuge for the characterization of detergent in solution, in: C. Wandrey, H. Cölfen (Eds.), Analytical Ultracentrifugation VIII., Springer, Place Published, 2006.
[29] P. Pernot, A. Round, R. Barrett, A. De Maria Antolinos, A. Gobbo, E. Gordon, J. Huet, J. Kieffer, M. Lentini, M. Mattenet, C. Morawe, C. Mueller-Dieckmann, S. Ohlsson, W. Schmid, J. Surr, P. Theveneau, L. Zerrad, S. McSweeney, Upgraded ESRF BM29 beamline for SAXS on macromolecules in solution, J. Synchrotron Radiat. 20 (2013) 660–664.
[30] M.V. Petoukhov, D. Franke, A.V. Shkumatov, G. Tria, A.G. Kikhney, M. Gajda, C. Gorba, H.D.T. Mertens, P.V. Konarev, D.I. Svergun, New developments in the ATSAS program package for small-angle scattering data analysis, J. Appl. Crystallogr. 45 (2012) 342–350.

[31] K. Mathieu, W. Javed, S. Vallet, C. Lesterlin, M.-P. Candusso, F. Ding, X.N. Xu, C. Ebel, J.-M. Jault, C. Orelle, Functionality of membrane proteins overexpressed and purified from E. coli is highly dependent upon the strain, Sci. Rep. 9 (2019) 2654.
[32] C. Breyton, W. Javed, A. Vermot, C.-A. Arnaud, C. Hajjar, J. Dupuy, I. Petit-Hartlein, A. Le Roy, A. Martel, M. Thépaut, C. Orelle, J.-M. Jault, F. Fieschi, L. Porcar, C. Ebel, Assemblies of lauryl maltose neopentyl glycol (LMNG) and LMNG-solubilized membrane proteins, Biochim. Biophys. Acta Biomembr. 1861 (2019) 939–957.
[33] P. Thebault, E. Taffin de Givenchy, M. Starita-Geribaldi, F. Guittard, S. Geribaldi, Synthesis and surface properties of new semi-fluorinated sulfobetaines potentially useable for 2D-electrophoresis, J. Fluor. Chem. 128 (2007) 211–218.
[34] Y. Chaudier, F. Zito, P. Barthélémy, D. Stroebel, B. Améduri, J.-L. Popot, B. Pucci, Synthesis and preliminary biochemical assessment of ethyl-terminated perfluoroalkylamine oxide surfactants, Bioorg. Med. Chem. Lett 12 (2002) 1587–1590.
[35] Y. Takeyama, Y. Ichinose, K. Oshima, K. Utimoto, Triethylborane-induced stereoselective radical addition of perfluoroalkyl iodides to acetylenes, Tetrahedron Lett. 30 (1989) 3159–3162.
[36] P.K. Mandal, J.S. Birtwistle, J.S. McMurray, Hydrodehalogenation of alkyl iodides with base-mediated hydrogenation and catalytic transfer hydrogenation: application to the asymmetric synthesis of N-protected α-methylamines, J. Org. Chem. 79 (2014) 8422–8427.
[37] S.H. Pine, B.L. Sanchez, Formic acid-formaldehyde methylation of amines, J. Org. Chem. 36 (1971) 829–832.
[38] V.M. Sadtler, M.P. Giulieri, K. M.P., J.G. Riess, Micellization and adsorption of fluorinated amphiphiles: questioning the 1CF2 ~1.5CH2 rule, Chem. Eur J. 4 (1998) 1952–1957.
[39] F. Mahler, A. Meister, C. Vargas, G. Durand, S. Keller, Self-assembly of protein-containing lipid-bilayer nanodiscs from small-molecule amphiphiles, Small 17 (2021), 2103603.
[40] E. Steinfels, C. Orelle, J.-R. Fantino, O. Dalmas, J.-L. Rigaud, F. Denizot, A. Di Pietro, J.-M. Jault, Characterization of YvcC (BmrA), a multidrug ABC transporter constitutively expressed in Bacillus subtilis, Biochemistry 43 (2004) 7491–7502.
[41] D. Lacabanne, C. Orelle, L. Lecoq, B. Kunert, C. Chuilon, T. Wiegand, S. Ravaud, J.-M. Jault, B.H. Meier, A. Böckmann, Flexible-to-rigid transition is central for substrate transport in the ABC transporter BmrA from Bacillus subtilis, Commun. Biol. 2 (2019) 149.
[42] C. Hajjar, M.V. Cherrier, G. Dias Mirandela, I. Petit-Hartlein, M.J. Stasia, J.C. Fontecilla-Camps, F. Fieschi, J. Dupuy, The NOX family of proteins is also present in bacteria, mBio 8 (2017) e01487-01417.
[43] M. Wehbie, I. Bouchemal, A. Deletraz, E. Pebay-Peyroula, C. Breyton, C. Ebel, G. Durand, Glucose-based fluorinated surfactants as additives for the crystallization of membrane proteins: synthesis and preliminary physical-chemical and biochemical characterization, ACS Omega 6 (2021) 24397–24406.